Atmospheric Environment 50 (2012) 164–173

Contents lists available at SciVerse ScienceDirect

Atmospheric Environment

journal homepage: www.elsevier.com/locate/atmosenv

Summertime aerosol chemical composition in the Eastern Mediterranean and its sensitivity to temperature

Ulas Im[a], Kostas Markakis[b], Mustafa Koçak[c], Evangelos Gerasopoulos[d], Nikos Daskalakis[a], Nikolaos Mihalopoulos[a], Anastasia Poupkou[b], Tayfun Kındap[e], Alper Unal[e], Maria Kanakidou[a,*]

[a] Environmental Chemical Processes Laboratory, Department of Chemistry, University of Crete, Voutes Campus, P.O. Box 2208, 71003 Heraklion, Greece
[b] Laboratory of Atmospheric Physics, Department of Physics, Aristotle University of Thessaloniki, Thessaloniki, Greece
[c] Institute of Marine Sciences, Middle East Technical University, Erdemli, Mersin, Turkey
[d] Institute for Environmental Research and Sustainable Development, National Observatory of Athens, Athens, Greece
[e] Eurasia Institute of Earth Sciences, Istanbul Technical University, Istanbul, Turkey

ARTICLE INFO

Article history:
Received 22 June 2011
Received in revised form
9 November 2011
Accepted 16 December 2011

Keywords:
Aerosol chemical composition
Temperature change
Eastern Mediterranean
Megacity

ABSTRACT

The impact of ambient temperature on the levels and chemical composition of aerosols over the Eastern Mediterranean in July 2004 is investigated using the WRF/CMAQ model system coupled with the MEGAN biogenic emissions model. CMAQ is able to capture the observed mean aerosol concentrations over the studied period. Non-sea-salt sulfate (nss-SO_4^{2-}) is calculated to be the major aerosol component contributing by 63%, 16% and 40% to the fine ($PM_{2.5}$), coarse ($PM_{2.5-10}$) and total particulate matter mass (PM_{10}), respectively. $PM_{2.5}$ to PM_{10} mass ratios reach more than 80% over the large urban agglomerations but decrease to 45% at downwind locations suggesting coagulation and condensation on coarse particles. Higher temperatures increase biogenic emissions, enhance spatially-averaged biogenic secondary organic aerosol (SOA, by $0.01 \pm 0.00\ \mu g\ m^{-3}\ K^{-1}$) and nitrate ($NO_3^-$) aerosol concentrations (by $0.02 \pm 0.02\ \mu g\ m^{-3}\ K^{-1}$). They reduce nss-$SO_4^{2-}$ (by $-0.04 \pm 0.07\ \mu g\ m^{-3}\ K^{-1}$), induced by significant reduction in the cloud cover (90% K^{-1}) and subsequent aqueous-phase production. The $PM_{2.5}$ concentrations show a very small positive response to temperature changes, increasing by $0.003 \pm 0.042\ \mu g\ m^{-3}\ K^{-1}$ (0.04% K^{-1}) due to the compensation of organic carbon increases by nss-SO_4^{2-} reductions. Locally, larger changes are computed, with nss-SO_4^{2-} and NO_3^- in fine aerosols reduced by up to $0.62\ \mu g\ m^{-3}\ K^{-1}$ and $0.80\ \mu g\ m^{-3}\ K^{-1}$, respectively. Increases as high as $0.097\ \mu g\ m^{-3}\ K^{-1}$ and $0.034\ \mu g\ m^{-3}\ K^{-1}$ are calculated for organic and elemental carbon, respectively. Results show that changes in temperature modify not only the aerosol mass but also its chemical composition.

1. Introduction

During the past decades considerable attention has been given to the understanding of the impact of aerosols on human health, climate, atmospheric chemistry and visibility. Aerosols are related to respiratory and cardiovascular diseases as well as to mortality (Schwartz et al., 1996; Bernard et al., 2001). They have direct and indirect effects on climate (IPCC, 2007). In turn, climate has a significant impact on aerosol concentrations (Jacob and Winner, 2009). Aerosols have both anthropogenic (e.g. transport and biomass burning) and natural sources (e.g. sea-salt, soil dust and vegetation). They are emitted as primary aerosols or are chemically formed from gaseous aerosol precursors in the atmosphere. Among a number of meteorological variables, changes in temperature and atmospheric water cycle can lead to changes in the levels and chemical composition of aerosols (Tsigaridis et al., 2005). Temperature and cloud droplet availability affect aqueous-phase non-sea-salt sulfate (nss-SO_4^{2-}) formation (Seinfeld and Pandis, 2006). Secondary organic aerosol (SOA) production through the oxidation of biogenic non-methane volatile organics (BVOC) is also affected by temperature. Temperature affects both the BVOC emissions and oxidation as well as the evaporation of the semi-volatile oxidation products in the aerosol phase and gas-to-particle partitioning (Tsigaridis and Kanakidou, 2007). Furthermore, temperature changes modify the atmospheric water cycle (including cloud formation and precipitation) and thus, the wet deposition (Dawson et al., 2007). Transport patterns can also change depending on the temperature. For example, updraft of pollutants to higher altitudes, characterized by stronger winds, would allow transport of pollutants to longer distances.

In the Eastern Mediterranean, the observed high ozone (O_3) and particulate matter (PM) levels often exceed the allowed limits

---

* Corresponding author. Tel.: +30 2810 545033; fax: +30 2810 545166.
E-mail address: mariak@chemistry.uoc.gr (M. Kanakidou).

1352-2310/$ – see front matter © 2011 Elsevier Ltd. All rights reserved.
doi:10.1016/j.atmosenv.2011.12.044

(e.g. Lazaridis et al., 2005; Gerasopoulos et al., 2006; Theodosi et al., 2010; Im et al., 2010). These exceedences are due to the contribution of anthropogenic and natural emissions surrounding the region, the important urban center emissions in the area, the regional biogenic emissions and the Mediterranean climate that favor photochemical production of secondary pollutants like O_3, nss-SO_4^{2-} and SOA (Kanakidou et al., 2011). The Eastern Mediterranean is particularly sensitive to climate change (IPCC, 2007) and is expected to be exposed to higher levels of pollutants in the future (Im et al., 2011). However, modeling studies of the impacts of climate change on air pollution in the region remain lacking. Recently, regional model simulations of future climate based on the IPCC A2 scenario (Carvalho et al., 2010) indicated decreases in PM_{10} levels up to 8 $\mu g\ m^{-3}$ in most of southern Europe and parts of the Eastern Mediterranean. Im et al. (2011) simulated the impact of air temperature increases on gaseous pollutants, including O_3, due to biogenic emissions and chemistry changes in the Eastern Mediterranean. The present modeling study builds upon that earlier work on gaseous air pollutants. It further evaluates the capability of the model system in simulating the aerosol levels and analyzes the mass concentration and chemical composition of aerosols in the Eastern Mediterranean and how they are affected by air temperature increases.

2. Materials and methods

2.1. Model system

The atmospheric modeling system used for this study consists of the Weather Research and Forecasting model (WRF-ARW v3.1.1; Skamarock and Klemp, 2008) online coupled with the Model of Emissions of Gases and Aerosols from Nature (MEGAN; Guenther et al., 2006) module of the WRF-CHEM 3.1.1 (Grell et al., 2005) for biogenic emissions, and off-line coupled with the U.S. EPA Community Multiscale Air Quality (CMAQ) model, v4.7 (Byun and Schere, 2006). The mesoscale model domain is shown in Fig. 1. The adopted model configurations, physical and chemical options, together with initial and boundary conditions are described in detail in Table S1 (also in Im et al., 2011). The anthropogenic emissions for the studied region are compiled using INERIS emissions for Europe to which, emissions for Greece on 10 km and for Istanbul and Athens on 2 km horizontal resolutions have been merged (Im et al., 2011 and references within). The global chemistry transport model TM4-ECPL (Myriokefalitakis et al., 2008, 2010) provides the initial and boundary conditions for the chemical tracers on a 6° × 4° horizontal resolution. Hereafter, we provide additional details on the aerosol modeling.

CMAQ model uses an aerosol component that is derived from the Regional Particulate Model (Binkowski and Shankar, 1995), which considers a modal representation of aerosols (Binkowski and Roselle, 2003) and the ISORROPIA v1.7 thermodynamic equilibrium model (Nenes et al., 1998) that accounts for the major ions but not for the crustal species of calcium, magnesium and potassium. CMAQ calculates the aerosol species in Aitken, accumulation and coarse modes as classified by Whitby (1978). Fine ($PM_{2.5}$: diameter $\geq$ 2.5 μm), coarse ($PM_{2.5-10}$: 2.5 μm $<$ diameter $\leq$ 10 μm) and total (PM_{10}: diameter $\leq$ 10 μm) mass concentrations are calculated during post processing of the individual aerosol components simulated at each model time step. Aerosol mass transfer from the accumulation to the coarse mode during atmospheric aging is taken into account based on the geometric mean diameters and standard deviations for the 2 considered lognormal modes. Anthropogenic $PM_{2.5}$ emissions used in CMAQ (primary organic carbon (POC), elemental carbon (EC), nss-SO_4^{2-}, nitrate (NO_3^-) and fine unspecified material) are speciated following the CARB (2007) chemical splitting profiles. The $PM_{2.5-10}$ emissions consist of natural sea-salt and anthropogenic PM. CMAQ

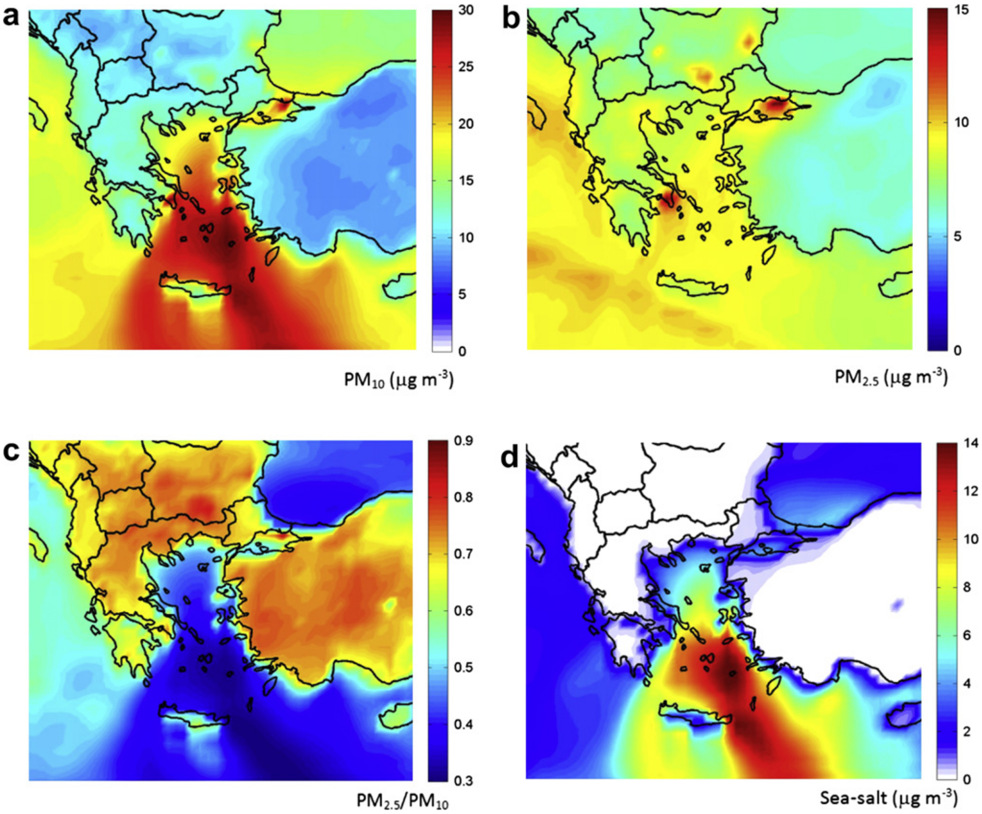

Fig. 1. Spatial distribution of predicted a) PM_{10}, b) $PM_{2.5}$, c) $PM_{2.5}/PM_{10}$ ratio and d) sea-salt calculated for the surface layer and averaged over the 15-day simulation period (1–15/7/2004).

internally assigns 90% of the anthropogenic primary $PM_{2.5-10}$ mass to fugitive dust (including re-suspension) and 10% to other unspecified material (Binkowski and Roselle, 2003). The desert dust fluxes are only provided from the boundaries extracted from the TM4-ECPL global model simulations on a monthly basis. Global dust emissions developed for the AEROCOM intercomparison model exercise (Dentener et al., 2006) and updated by Vignati E. (personal communication, 2010) to account for the year 2008 have been used in TM4-ECPL. Regional natural dust emissions are not taken into account. The sea-salt emissions are computed online based on wind speed at 10 m (Gong, 2003) and applying a size correction due to relative humidity changes (Zhang et al., 2005). Only the open-sea emissions of sea-salt are here considered, possibly leading to significant underestimations by neglecting emissions from coastal areas (de Leeuw et al., 2000; Matthias et al., 2008; Kelly et al., 2010). Marine POC (Myriokefalitakis et al., 2010 and references therein) and Dimethylsulfide (DMS) emissions are here neglected.

The aerosol module (AERO5) accounts for heterogeneous N_2O_5 hydrolysis and SOA formation (Foley et al., 2010). AERO5 also simulates sulfuric acid condensation on $PM_{2.5-10}$ and semi-volatile inorganic species (ammonia, nitric acid and hydrochloric acid) condensation on/evaporation from $PM_{2.5-10}$. SOA in AERO5 is formed during isoprene, sesquiterpenes and benzene oxidation in the gas phase and glyoxal and methylglyoxal oxidation in the aqueous phase (Carlton et al., 2010).

The Integrated Process Analysis (IPR) tool of the CMAQ model has been employed to identify the contributions of the main physical and chemical processes controlling the levels of the major aerosol components. The processes that are here investigated are: horizontal and vertical transport, emissions of primary species, gas-phase chemistry, dry deposition, cloud processes and aerosol processes (particle formation, condensation, coagulation and aerosol thermodynamics: Im et al., 2011).

2.2. Simulations

Seven scenarios have been simulated to evaluate the model performance and the impact of air temperature changes on aerosol concentrations in the Eastern Mediterranean. All simulations have been conducted for a 26-day period (June 20 to July 15, 2004). This period has been selected based on the availability of observations including isoprene at Finokalia station on Crete. The period is also characterized by dominant northerly winds, which are typical for summertime conditions in the region. These winds minimize Sahara dust impacts in the region and maximize outflow from Istanbul and Athens over the Aegean and the East Mediterranean seas (Im et al., 2011). The first 11 days have been used as a spin-up period in order to reach a chemical equilibrium for both gases and aerosols and have not been evaluated in the analyses. Scenarios S1 to S5 have been performed to calculate the impacts of homogeneous increases in ambient temperatures by 1–5 K on aerosols compared to the base case simulation (S0). Temperature perturbations have been applied in two steps: First, the biogenic emissions have been calculated by the MEGAN model using surface temperatures increased by +1 K (S1) to +5 K (S5) compared to the temperatures in S0. Second, the Meteorology–Chemistry Interface Processor (MCIP: Otte and Pleim, 2010) output has been modified by increasing air temperatures throughout the modeling domain. It is then used to drive meteorology in the CMAQ model. Changes in evaporative VOC anthropogenic emissions have been neglected. The last temperature scenario (S6) has been performed to investigate the impact of air temperatures from a warmer year (July 2007) on aerosols in the area. An important feature of S6 is that the meteorology is recalculated with the WRF model based on perturbed ambient temperatures. Thus, this scenario is also characterized by changes in most meteorological variables. In addition to soil moisture and temperature, winds and clouds are also different in S6 (Im et al., 2011). Scenario S6 applies lower temperatures over land than S0 and thus, lower biogenic emissions are calculated (Im et al., 2011). Further details on these simulations are provided in Im et al. (2011).

3. Results and discussion

3.1. Base case analyses

3.1.1. Spatial distribution

The spatial distributions of PM_{10}, $PM_{2.5}$ and $PM_{2.5}/PM_{10}$ mass ratios in the surface model layer, averaged for the 15-day simulation, are presented in Fig. 1. Fig. 1a and b clearly depict the dominance of $PM_{2.5}$ that is characterizing the Istanbul and Athens extended areas. The $PM_{2.5}/PM_{10}$ mass fractions (Fig. 1c) are higher than 0.7 near the urban agglomerations and decreases downwind, particularly over the regions where coarse sea-salt aerosol dominates. Sea-salt aerosol (Fig. 1d) extends from the central Aegean Sea to the Eastern Mediterranean. Fig. 1b also highlights the shipping contribution in the Aegean and Mediterranean seas to $PM_{2.5}$.

The spatial distributions of NO_3^-, organic carbon (OC), nss-SO_4^{2-} and the $PM_{2.5}/PM_{10}$ fraction of nss-SO_4^{2-} are shown in Fig. 2. The simulated nss-SO_4^{2-} levels are higher over the sea than over the land (Fig. 2a) due to the lower dry deposition (Fig. S1a) and to higher OH levels (Im et al., 2011) over the sea that enhance oxidation of sulfur dioxide (SO_2) from shipping. The in-cloud production of nss-SO_4^{2-} is also important over the western parts of the domain (Ionian Sea), where cloudiness is high (Fig. S1b). The $PM_{2.5}/PM_{10}$ mass fraction of nss-SO_4^{2-} (Fig. 2b) indicates significant nss-SO_4^{2-} levels in the coarse mode over the sea, pointing to interactions of sulfate with sea-salt and dust particles as previously reported for the region (Koçak et al., 2007). The NO_3^- levels are low over land and higher over the sea (Fig. 2c), mainly associated with the sea-salt aerosol. Indeed, NO_3^- and Na^+ are highly correlated both in modeling results (correlation (r) = 0.72, number of points (n) = 360) and in earlier reported observations in the region (Bardouki et al., 2003; r = 0.80; also references in Tables 1 and 2). The OC distribution clearly indicates Istanbul and Athens extended areas and the shipping routes in the Aegean and the Mediterranean seas (Fig. 2d).

3.1.2. Model evaluation

The calculated PM_{10} concentrations for the surface model layer have been evaluated by comparison with daily observations from Istanbul, Athens, Thessaloniki and Finokalia. For the study period, data are available from 6 stations in Istanbul (Air Quality Network of Istanbul Metropolitan Municipality; IST), 5 stations in Athens (National Air Pollution Monitoring Network of the Hellenic Ministry of Environment Energy and Climate Change; ATH), 1 station in Thessaloniki (Air Quality Monitoring Network of the Region of Central Macedonia; THES), and Finokalia station on Crete Island (University of Crete; Koulouri et al., 2008; FKL). Continuous aerosol observations are not available at FKL for the simulation period. The simulated PM_{10} concentrations are compared with the observations averaged over all stations that are located in the corresponding model grid. Geographical information for the monitoring stations and the statistics of the comparison between calculated and observed PM_{10} are presented in Table 1. The model poorly reproduces the temporal variability of the observations at ATH (r = 0.17) and IST (r = 0.32). On the other hand, it performs better for the urban stations in Athens (r = 0.52) and for THES (r = 0.75). The simulations overestimate the observations at IST by 27%, whereas they underestimate them at ATH by 27% and at THES by 67%. The calculated chemical composition of the PM_{10} (mass concentrations of nss-SO_4^{2-}, NO_3^-, NH_4^+, Na^+, EC and OC) is comparable with earlier

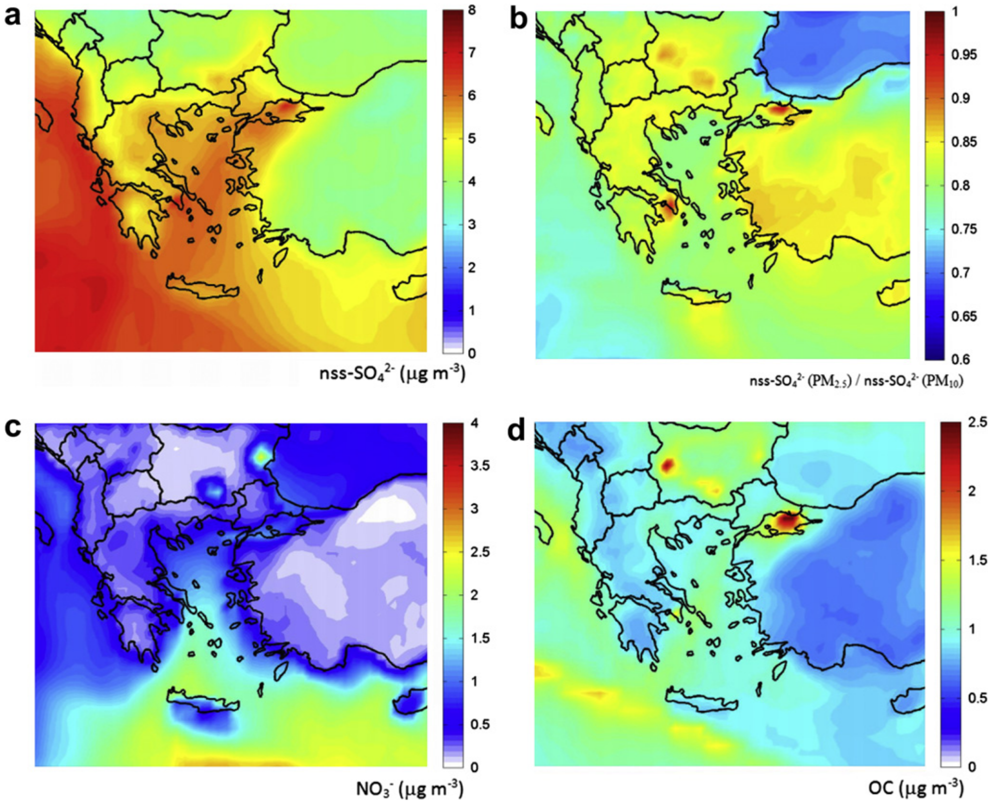

Fig. 2. Spatial distributions of surface a) nss-SO_4^{2-}, b) fine/coarse nss-SO_4^{2-} ratio, c) NO_3^- and d) OC concentrations averaged over the 15-day simulation period (1–15/7/2004).

observational and modeling studies in the region (Table 2). The variability of the reported observations may reflect differences in the location, time and procedure of sampling and the analytical methods applied.

The non-systematic (positive and negative) differences in NO_3^- and NH_4^+ (Table 2) can be mainly attributed to the high uncertainty in ammonia emissions, but also to uncertainties in the small amount of primary NO_3^- emissions. Considerably lower correlation coefficients between the fine mode NH_4^+ and nss-SO_4^{2-} ($r = 0.38$, slope in equivalents = 0.15) are calculated for FKL than observed (Mihalopoulos et al., 1997: $r = 0.91$, slope = 0.32; Koulouri et al., 2008: $r = 0.89$, slope = 0.85). This suggests underestimation of NH_4^+ neutralization by nss-SO_4^{2-}. Na^+ differences between the current and previous studies (Athanasopoulou et al., 2008) are attributed to the different meteorological conditions (wind speed, temperature and humidity) between the selected simulation periods. In addition, consideration of open-sea emissions of sea-salt only leads to underestimation of sea-salt emissions and those associated with coarse

Table 1
Geographical information for the air quality monitoring stations used to evaluate the model results and the statistics of the comparison between calculated and observed PM_{10} concentrations. *R*: Correlation coefficient; MNB: Mean normalized bias; RMSE: Root mean square error; IOA: Index of agreement (see details in Im et al., 2011).

Stations	Latitude	Longitude	Altitude (m asl)	Classification	R	BIAS (μg m^{-3})	MNB (%)	RMSE (μg m^{-3})	IOA
IST					0.32[a]	6.30	0.27	8.84	0.51
Alibeykoy	41.07	28.95	60	Urban					
Besiktas	41.05	29.01	94	Urban/Traffic					
Esenler	41.04	28.89	59	Urban					
Kadikoy	40.99	29.03	6	Urban					
Sariyer	41.70	29.05	103	Urban background					
Uskudar	41.02	29.03	70	Urban					
ATH					0.17[a]	−14.91	−0.27	21.42	0.50
Marousi	38.03	23.79	145	Urban/Traffic	0.52[b]	−2.64	−0.04	10.29	0.69
Aristoteleus	37.99	23.73	95	Urban/Traffic					
Lykovrysi	38.07	23.78	210	Suburban	0.38[c]	−6.30	−0.13	12.2	0.53
Zografou	37.97	23.79	245	Suburban background					
Ag. Paraskevi	37.99	23.82	290	Suburban background					
THES									
Panaroma	40.59	23.03	363	Suburban	0.75	−26.30	−0.67	28.18	0.39
FKL									
Finokalia	35.20	25.40	250	Remote	N/A	N/A	N/A	N/A	N/A

[a] Statistics for all stations.
[b] Statistics for urban stations in Athens.
[c] Statistics for suburban stations in Athens.

Table 2
Comparison of the PM_{10} composition ($\mu g\ m^{-3}$) calculated in the present study with previous studies in the region. Parentheses show the standard deviation (one number) or the minimum and maximum values (two numbers), if available.

Location	Period	nss-SO_4^{2-}	NO_3^-	NH_4^+	Na^+	EC	OC	Reference
Istanbul	1–31/7/08	3.4 (1.1)	0.7 (0.2)	0.3 (0.2)	3.1 (0.6)	2.5 (1.2)	4.8 (1.8)	Theodosi et al., 2010 (Obs.)
	1–15/7/04	6.4 (1.2)	0.8 (0.5)	2.1 (0.3)	0.4 (0.4)	2.6 (0.9)	6.9 (2.3)	This study
Athens	29/8–16/9/94	5.5 (3–10)	2 (1–5)	1.5 (0.5–4)	0.5			Eleftheriadis et al., 1998 (Obs.)
	24/6/98	5.8 (1)	0.4 (0.4)	1 (0.5)	0.8 (0.2)			Athanasopoulou et al., 2008 (Model)
	2/6/03–21/7/03	8.2 (1.1)	1.8 (0.7)	2.4 (0.4)		2.0 (0.5)	14.1 (1.9)	Sillanpaa et al., 2006 (Obs.)
	1–15/7/04	7.3 (1.4)	0.6 (0.2)	1.8 (0.4)	0.5 (0.4)	1.2 (0.5)	1.6 (0.5)	This study
Thessaloniki	7/97–7/98	7.2 (5.8)	3.4 (1.9)	3.5 (2.3)	0.6 (0.5)			Tsitouridou et al., 2003 (Obs.)
	24/6/98	13.4 (2.8)	0.2 (0.3)	2.2 (0.9)	0.6 (0.2)			Athanasopoulou et al., 2008 (Model)
	6/07–9/07	6.2 (1.7–13.6)	1.3 (0.3–4.1)	1.3 (0.2–4.2)	0.3 (0–1.8)	2.8 (1–7.7)	6.5 (2.8–23.7)	Terzi et al., 2010 (Obs.)
	1–15/7/04	6.6 (1.4)	0.4 (0.3)	1.8 (0.4)	0.1 (0.1)	0.3 (0.1)	1.0 (0.2)	This Study
Finokalia	13–16/7/00	4.2	3.4	1	4.1			Smolik et al., 2003 (Obs.)
	26–30/7/00	8.2	2	3.7	0.6			Smolik et al., 2003 (Obs.)
	10–31/7/00, 7–14/1/01	6.9 (1.0)	2.8 (0.4)	2.4 (0.4)	2.0 (0.3)	(0.1–0.7)	(0.3–2.2)	Bardouki et al., 2003 (Obs.)
	24/6/98	5.3 (1)	0.9 (0.3)	0.4 (0.1)	2.3 (0.8)			Athanasopoulou et al., 2008 (Model)
	12–16/7/04	8.1	2.1	2.3	1.1	0.6 (0.1)	4.7 (1.2)	Koulouri et al., 2008 (Obs.)
	12–15/7/04[a]	6.5 (1.4)	0.6 (0.3)	1.0 (0.2)	0.5 (0.4)	0.3 (0.1)	0.8 (0.2)	This Study
	1–15/7/04	6.8 (1.1)	1.1 (0.4)	1.1 (0.2)	1.2 (0.8)	0.3 (0.1)	0.9 (0.2)	This study

[a] 12–15/7/2004 period of our simulation is extracted from the 15-day simulation period in order to be compared with Koulouri et al. (2008).

mode NO_3^- aerosols (see section 2.1). Finally, Kouvarakis and Mihalopoulos (2002) showed that DMS account for about 1%–17% of the nss-SO_4^{2-} in the Eastern Mediterranean during winter and summer, respectively. Omission of DMS emissions contributes to differences between simulated and observed nss-SO_4^{2-} concentrations.

3.1.3. *Aerosol chemical composition*

The computed chemical compositions of the spatially-averaged fine and coarse fractions of PM show that 79% of nss-SO_4^{2-} and 81% of NH_4^+ reside in the fine mode as expected (Seinfeld and Pandis, 2006). In the region, nss-SO_4^{2-} is formed mainly through production of sulfuric acid (H_2SO_4) that has low vapor pressure and nucleates or condenses mainly on fine mode aerosols (Mihalopoulos et al., 2007) that contain most of the aerosol surface.

The calculated contribution of fine mode nss-SO_4^{2-} to the total nss-SO_4^{2-} (domain mean 79%; Fig. 2b) compares well with the observations by Koçak et al. (2007) and Koulouri et al. (2008) of 81% and 80%, respectively. Spatially-averaged nss-SO_4^{2-} is calculated to comprise 63% of $PM_{2.5}$, 15% of $PM_{2.5-10}$ and 40% of PM_{10}. NH_4^+ is mainly neutralizing nss-SO_4^{2-} and, thus, also resides in the fine mode (81% of total NH_4^+ mass) in agreement with observations by Koulouri et al. (2008) (89% of NH_4^+ fine mass fraction).

In contrast, NO_3^-, Na^+ and Cl^- reside predominantly in the coarse mode with calculated domain mean coarse-to-total fractions of 94%, 93% and 96%, respectively, comparable to the ~90% observed by Koçak et al. (2004) and Koulouri et al. (2008). Na^+ shows strong correlation with NO_3^- both in the model ($r = 0.72$) and in the observations (e.g. $r = 0.80$ at FKL, Bardouki et al., 2003).

Natural sources also contribute significantly to PM_{10} mass. Spatially-averaged sea-salt and dust contributions are 20% and 15%, respectively. This dust contribution is comparable with, although slightly lower than, the 25–35% observed by Gerasopoulos et al. (2006) during non-dust periods in spring and fall. It is also comparable with the model calculated annual means of 20% and 19–25% simulated by Mitsakou et al. (2008) and Papanastasiou et al. (2010), respectively. The difference from earlier studies can be attributed both to the interannual variability of dust and to the representation of the natural dust fluxes in the present study by the boundary conditions only (see Section 2.1). Nevertheless, northerly winds that dominated during the simulated period minimized the impact of Sahara dust transport to the region. In addition, local anthropogenic dust can be a significant source in the region. Karanasiou et al. (2011) calculated a road dust contribution of 29% and soil dust contribution of 19% to the PM_{10} levels in Madrid in summer 2009, very close to the 21% calculated by Nicolas et al. (2008) for local dust contribution in the Madrid area. The observational data analysis by Koçak et al. (2011) evaluated the total traffic contribution (including road dust) to the PM_{10} levels in Istanbul at 18.9%.

Biogenic SOA (bSOA) contributes more to the PM_{10} mass at THES and FKL than at IST and ATH where anthropogenic emissions are the major drivers of SOA. Domain-wide, bSOA contributes (1.4%) to the PM_{10} mass, 3 times more than the anthropogenic SOA (aSOA: 0.4%). Primary organic aerosols (POA) emitted from anthropogenic urban sources contribute by 98%, 90%, 84% and 85% to the total OC at IST, ATH, THES and FKL, respectively, indicating major anthropogenic influence for this aerosol component. Chemical aging of organic aerosol (OA) is of importance for the formation of oxygenated OA that is considered as SOA (Jimenez et al., 2009) and is not included in the present study. The applied CMAQ configuration makes use of the CB05 mechanism and does not explicitly account for long-chain alkane chemistry (Carlton et al., 2010). In highly polluted urban areas, alkanes can be a significant fraction (~40–45%) of non-methane volatile organic compounds (NMVOC) as has been observed by Arsene et al. (2009) for the Eastern Mediterranean atmosphere. This omission could explain the calculated high POA compared to SOA and the underestimation of OA by the model (Table 2).

Significant differences in the aerosol chemical composition are computed between the urban agglomerations and the downwind locations. Fig. 3 depicts the contributions of major aerosols to the $PM_{2.5}$ and $PM_{2.5-10}$ masses at the urban site IST and at the downwind site FKL. In the megacity $PM_{2.5}$ consists largely of POA (27%) and unspecified anthropogenic particles (28%), whereas at FKL these contributions are only 9 and 4%, respectively. Furthermore at FKL, the inorganic fine aerosol content is higher than the unspecified PM (Fig. 3). Thus, the nss-SO_4^{2-} contribution to the $PM_{2.5}$ mass is much lower in the megacity (24%), where anthropogenic primary nss-SO_4^{2-} exists (section 2.1), than at the receptor site (65%), where it actually dominates fine particles due to chemical formation during transport (Fig. 3). At ATH, the nss-SO_4^{2-} contribution to the $PM_{2.5}$ mass is 30% (6.8 $\mu g\ m^{-3}$), close to that of IST, whereas at THES it is almost double although similar in mass concentration (5.6 $\mu g\ m^{-3}$; 61%). The simulated nss-SO_4^{2-} mass concentration at FKL (5.7 $\mu g\ m^{-3}$) compares well with the observed 6.1 $\mu g\ m^{-3}$ although the relative contribution to $PM_{2.5}$ (65%) overestimates the observations (37%) by Lelieveld et al. (2002). This can result from an

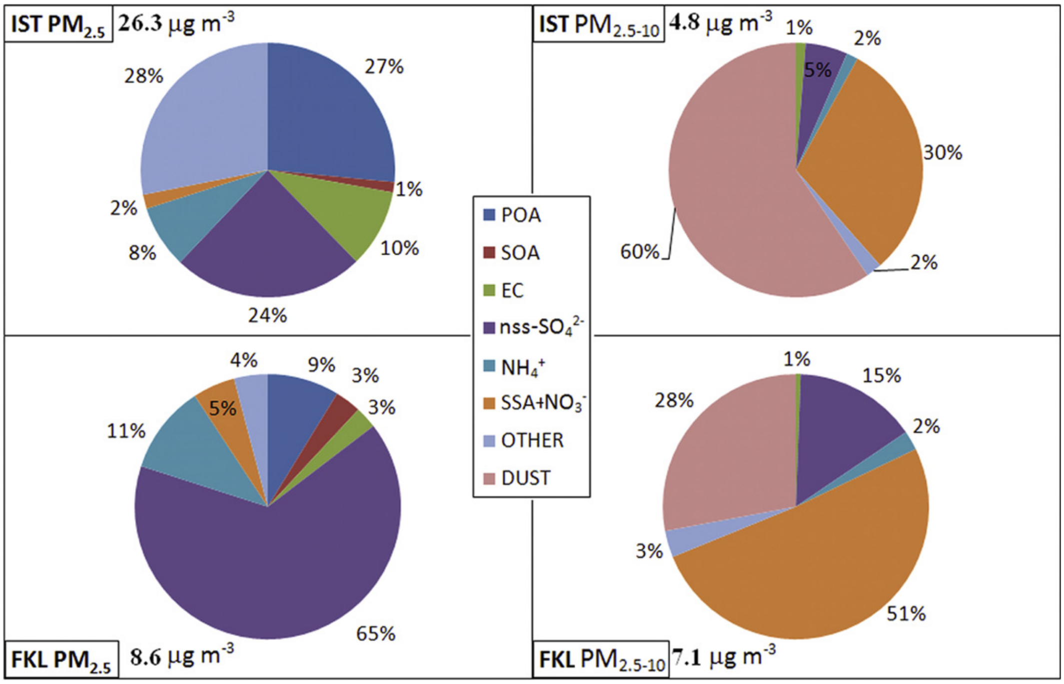

Fig. 3. Surface contributions of aerosol species to total $PM_{2.5}$ and $PM_{2.5-10}$ mass at IST and FKL, averaged over the 15-day simulation period (1–15/7/2004) and model domain (E. Mediterranean).

underestimation in the $PM_{2.5}$ caused by the significantly lower OA mass calculated than observed. Indeed in the remote atmosphere, as discussed earlier, OA is significantly underestimated by the model (~1 $\mu g\ m^{-3}$) compared with 5.2 $\mu g\ m^{-3}$ and 4.7 $\mu g\ m^{-3}$ observed by Lelieveld et al. (2002) and Koulouri et al. (2008), respectively (Table 2). Elemental carbon (EC) is higher in the megacity (10%) than at the receptor site (3%), showing local anthropogenic urban sources and removal during transport to FKL. The OC/EC ratios calculated for IST (2.72) and for FKL (4.44) also point to a higher anthropogenic contribution at IST. In Athens, EC is much lower (1.2 $\mu g\ m^{-3}$; 5%). POA at ATH is also calculated to be much lower than at IST (1.4 $\mu g\ m^{-3}$; 6%). THES exhibits even lower POA and EC concentrations (0.9 $\mu g\ m^{-3}$, 9%, and 0.3 $\mu g\ m^{-3}$, 3%, respectively).

The main changes in the coarse aerosol ($PM_{2.5-10}$) from the urban to the downwind sites originate from the natural aerosols. The sea-salt contribution to $PM_{2.5-10}$ increases from 23% (1.1 $\mu g\ m^{-3}$) at the coastal urban site (IST) to 44% (3.1 $\mu g\ m^{-3}$) at the coastal downwind site (FKL) whereas the dust contribution decreases from 60% (3.0 $\mu g\ m^{-3}$) at IST to 28% at FKL (2.0 $\mu g\ m^{-3}$). The dust variability in the model results from boundary flux changes driven by meteorology and due to re-suspended dust (Section 2.1). The coarse mode nss-SO_4^{2-} contribution increases from 5% (0.3 $\mu g\ m^{-3}$) at IST to 15% (1.1 $\mu g\ m^{-3}$) at FKL, which indicates an acid displacement mechanism that moves part of SO_4^{2-} to coarse sea-salt aerosols during transport over the Aegean Sea. The coarse mode nss-SO_4^{2-} concentration of 1.1 $\mu g\ m^{-3}$ calculated by the model is comparable to the 1.5 $\mu g\ m^{-3}$ observed by Lelieveld et al. (2002). However, dust and sea-salt concentrations calculated for July 2004 are underestimated compared to observations by Lelieveld et al. (2002) in summer 2001.

3.2. Scenario analyses

3.2.1. Temperature effects on aerosol spatial distribution

In order to investigate the effect of temperature changes on aerosol mass spatial distributions, the differences in $PM_{2.5}$ in scenarios S5 and S6 compared to scenario S0, averaged over the 15-day simulation period, were calculated and these are shown in Fig. 4 and S2. The simulated spatially-averaged masses of the major fine and coarse aerosol components for all scenarios are presented in Table 3. $PM_{2.5}$ concentrations increase by 0.015 $\mu g\ m^{-3}$ (0.2%) in S5 (temperatures enhanced by 5 K, Fig. 4a) and decrease by 0.941 $\mu g\ m^{-3}$ (15%, Fig. S2a) in S6 compared to S0. The different responses in S6 are due to differences in the meteorology (Section 2.2). For scenarios S0 to S5, the spatially-averaged changes in $PM_{2.5}$ concentrations are calculated to be 0.003 ± 0.042 $\mu g\ m^{-3}\ K^{-1}$ (0.04% K^{-1}). This large standard deviation indicates a significant spatial variability in the $PM_{2.5}$ response to temperature changes. Locally, fine mode nss-SO_4^{2-} and NO_3^- are reduced by up to 0.62 $\mu g\ m^{-3}\ K^{-1}$ and 0.80 $\mu g\ m^{-3}\ K^{-1}$, respectively, whereas increases as high as 0.097 $\mu g\ m^{-3}\ K^{-1}$ and 0.034 $\mu g\ m^{-3}\ K^{-1}$ are calculated for organic and elemental carbon, respectively. For S5, the increases in the fine mode are mostly over the sea (Fig. 4a) and are mainly due to changes in nss-SO_4^{2-}, NH_4^+ and OC concentrations (Fig. 4b,c,d). On the other hand, the $PM_{2.5}$ changes in S6 (Fig. S2a) are mostly attributed to changes in OC concentrations (Fig. S2d). Positive changes are calculated for NO_3^- that resides mainly on $PM_{2.5-10}$ and is associated with the coarse sea-salt and dust particles.

3.2.2. Temperature driven changes in aerosol chemical composition

Since the environmental impact of aerosols also depends on their chemical composition, the impact of temperature changes on the chemical composition of the aerosols is further investigated. Fig. 5 depicts the relative contributions of the main aerosol components to the total $PM_{2.5}$ and $PM_{2.5-10}$ masses for scenarios S0, S5 and S6, averaged over the simulation domain and period. Decreases in the fine mode nss-SO_4^{2-} concentrations (Fig. 5a, c, e) by 0.22 (4%) and 0.72 $\mu g\ m^{-3}$ (14%) are calculated in S5 and S6, respectively. These can be mainly attributed to a reduction in the aqueous-phase production of nss-SO_4^{2-} (by 0.06 ± 0.1 $\mu g\ m^{-3}\ K^{-1}$ (31%)) in the entire PBL due to the significant reduction in the domain-mean non-precipitating cloud fraction (NP_CLDFRAC) by ~90% K^{-1} (Table 3). In scenario S6, an increase of 77% in precipitating cloud fractions is calculated, causing an 80% increase in the

Table 3

Domain- and simulation-averaged concentrations of major aerosol and gas species for each scenario and ΔC/ΔT for S1 to S5 (mean and standard deviation in parenthesis in $\mu g\ m^{-3}\ K^{-1}$) and for S6 (in $\mu g\ m^{-3}$).

	S0	S1	S2	S3	S4	S5	S6	ΔC/ΔT in S1–S5	ΔC in S6
PM_{10} ($\mu g\ m^{-3}$)	16.437	16.448	16.458	16.527	16.596	16.643	16.698	0.041 (0.029)	0.261
$PM_{2.5-10}$ ($\mu g\ m^{-3}$)	8.213	8.253	8.304	8.342	8.380	8.404	9.415	0.038 (0.009)	1.202
$PM_{2.5}$ ($\mu g\ m^{-3}$)	8.224	8.154	8.154	8.185	8.216	8.239	7.283	0.003 (0.042)	−0.941
nss-$SO_{4\ 2.5-10}$ ($\mu g\ m^{-3}$)	1.359	1.222	1.183	1.172	1.161	1.150	1.127	−0.042 (0.055)	−0.233
nss-$SO_{4\ 2.5}$ ($\mu g\ m^{-3}$)	5.229	5.065	5.014	5.014	5.014	5.010	4.510	−0.044 (0.070)	−0.719
$NO_{3\ 2.5-10}$ ($\mu g\ m^{-3}$)	0.875	0.930	0.951	0.966	0.981	0.992	0.901	0.024 (0.018)	0.027
$NO_{3\ 2.5}$ ($\mu g\ m^{-3}$)	0.061	0.061	0.060	0.060	0.060	0.062	0.057	0.000 (0.000)	−0.004
$NH_{4\ 2.5-10}$ ($\mu g\ m^{-3}$)	0.279	0.265	0.259	0.256	0.253	0.250	0.218	−0.006(0.005)	−0.061
$NH_{4\ 2.5}$ ($\mu g\ m^{-3}$)	1.169	1.184	1.186	1.186	1.189	1.185	1.006	0.032 (0.007)	−0.163
$Na_{2.5-10}$ ($\mu g\ m^{-3}$)	1.151	1.213	1.244	1.261	1.278	1.291	1.582	0.028 (0.020)	0.431
$Na_{2.5}$ ($\mu g\ m^{-3}$)	0.089	0.099	0.107	0.112	0.116	0.120	0.121	0.006 (0.003)	0.032
$Cl_{2.5-10}$ ($\mu g\ m^{-3}$)	1.541	1.617	1.657	1.675	1.693	1.708	2.281	0.035 (0.026)	0.740
$Cl_{2.5}$ ($\mu g\ m^{-3}$)	0.061	0.072	0.080	0.086	0.092	0.097	0.089	0.007 (0.002)	0.028
Sea-salt ($\mu g\ m^{-3}$)	3.216	3.405	3.504	3.560	3.615	3.659	4.417	0.089 (0.006)	1.202
$H_2O_{2.5-10}$ ($\mu g\ m^{-3}$)	10.651	9.302	8.296	7.607	6.917	6.437	13.446	−0.843 (0.340)	2.795
$H_2O_{2.5}$ ($\mu g\ m^{-3}$)	9.559	7.131	5.899	5.205	4.511	4.022	7.284	−1.107 (0.788)	−2.275
aSOA ($\mu g\ m^{-3}$)	0.062	0.063	0.062	0.061	0.061	0.060	0.048	−0.000 (0.000)	−0.015
bSOA ($\mu g\ m^{-3}$)	0.232	0.242	0.259	0.269	0.279	0.290	0.180	0.012 (0.003)	−0.052
OC ($\mu g\ C\ m^{-3}$)	0.986	1.004	1.016	1.022	1.029	1.035	0.887	0.010 (0.005)	−0.100
ORGPAT ($\mu g\ m^{-3}$)[a]	0.839	0.851	0.855	0.857	0.858	0.860	0.772	0.004 (0.005)	−0.067
Dust ($\mu g\ m^{-3}$)	2.490	2.463	2.455	2.452	2.449	2.443	2.589	−0.010 (0.010)	0.099
PR_CLD_FRAC[b]	0.003	0.003	0.003	0.003	0.003	0.003	0.005	−3.50 (4.33)	76.67
NP_CLD_FRAC[b]	0.011	0.002	2.68E-4	3.67E-5	2.45E-6	4.81E-8	0.012	−89.40 (6.02)	7.02

S0 denotes the base case scenario while S1 to S5 denote temperature increases from 1 to 5 K and S6 denotes the recalculated meteorology based on July 2007 temperatures.

[a] ORGPAT denotes primary anthropogenic organic aerosols.

[b] PR_CLD_FRAC and NP_CLD_FRAC denote precipitating and non-precipitating cloud fractions, respectively.

wet deposition removal of nss-SO_4^{2-} domain wide. Temperature increases between 1 and 5 K change the spatially-averaged fine mode nss-SO_4^{2-} concentration by −0.04 ± 0.07 $\mu g\ m^{-3}\ K^{-1}$ (−0.9% K^{-1}).

In contrast, the fine mode NH_4^+ increases by 0.03 ± 0.01 $\mu g\ m^{-3}\ K^{-1}$ (0.3% K^{-1}) due to an increase in the production of ammonium bisulfate (NH_4HSO_4) aerosol, as previously suggested by Mihalopoulos et al. (1997). The model calculated NH_4^+/nss-SO_4^{2-} molar ratios are

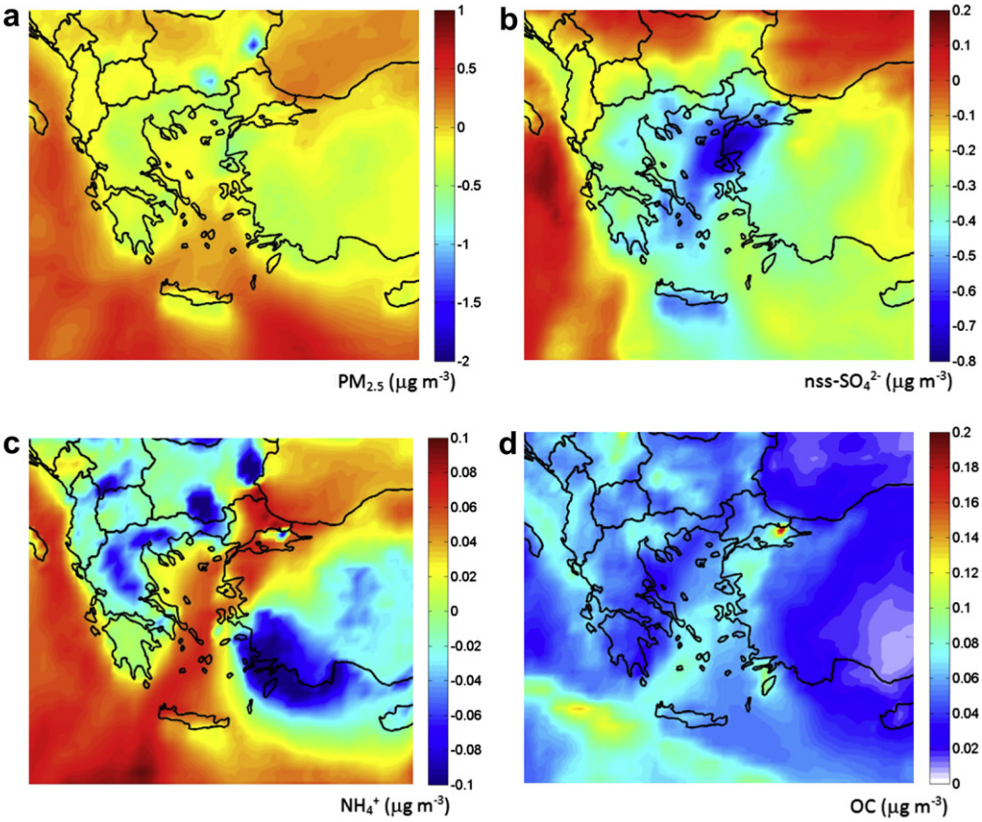

Fig. 4. Absolute changes in spatial distribution of fine mode a) $PM_{2.5}$, b) nss-SO_4^{2-}, c) NH_4^+, and d) OC concentrations in the lowest model layer in scenario S5 (+5 K) relative to the scenario S0 (base case), averaged over the 15-day simulation period, Additional information is given in Table 3 and Section 2.2.

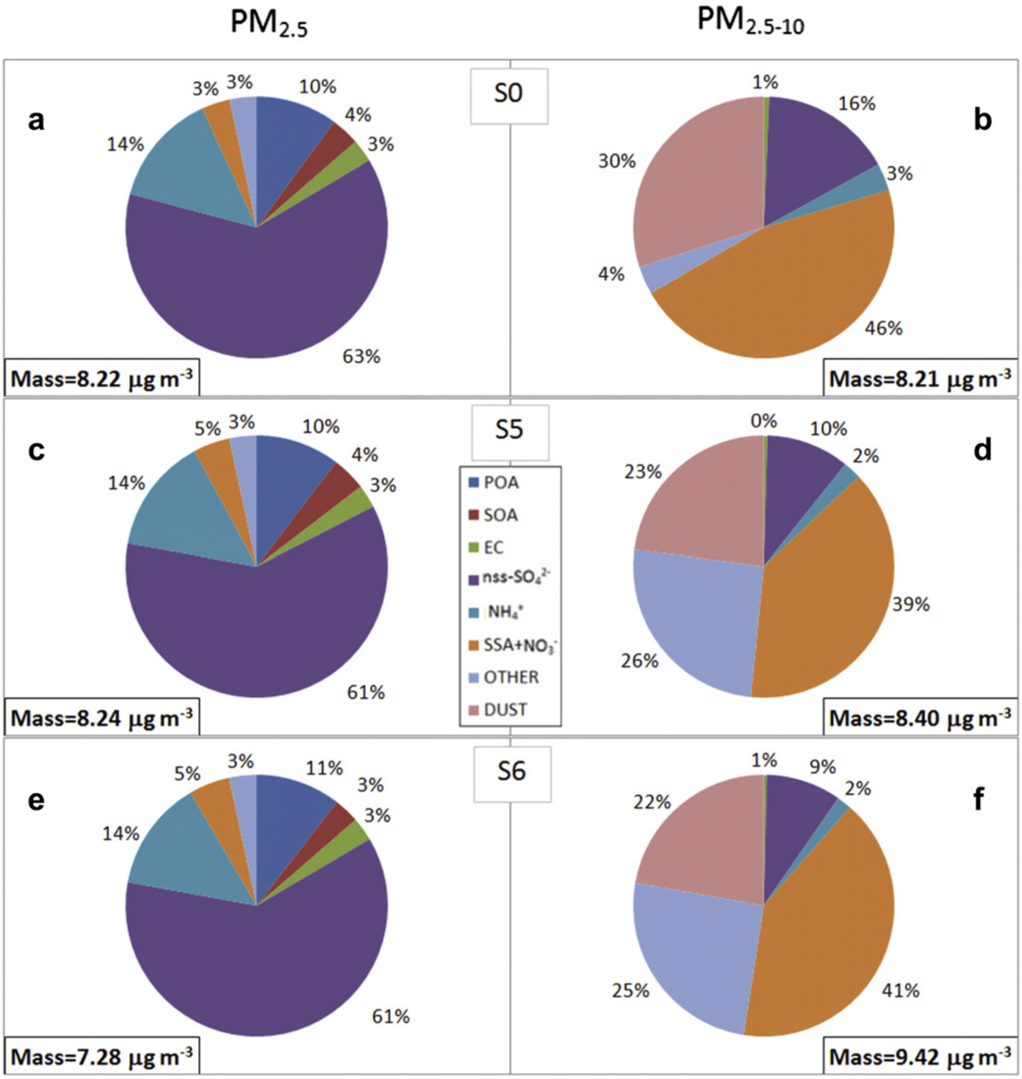

Fig. 5. Surface contributions of major aerosol species to total $PM_{2.5}$ and $PM_{2.5-10}$ masses in scenarios S0 (base case), S5 (+5 K) and S6 (2007 temperatures), averaged over the 15-day simulation period (1–15/7/2004) and the model domain (E. Mediterranean) Additional information is given in Table 3 and Section 2.2.

slightly above one (~1.1) in all scenarios with an increasing trend with increasing temperatures. SOA concentrations increase in scenarios S1 to S5, due to higher emissions of isoprene, monoterpene and sesquiterpene by 9% K^{-1}, 11% K^{-1}, and 19% K^{-1}, respectively (Im et al., 2011). As a consequence, the domain- and simulation-mean bSOA concentrations are enhanced by 0.06 $\mu g\ m^{-3}$ (25%) over the model domain in scenario S5 and by 0.01 ± 0.00 $\mu g\ m^{-3}\ K^{-1}$ (5% K^{-1}) in scenarios S1 to S5. In scenario S6, bSOA concentrations decrease by 0.05 $\mu g\ m^{-3}$ (22%) due to the reduction in biogenic emissions (Im et al., 2011). The fine mode sea-salt + NO_3^- concentrations increase in all scenarios, as seen in Fig. 5a, c and e, due to the increase in sea-salt emissions by ~1.6% K^{-1}. The fine mode sea-salt + NO_3^- for S1 to S5 is calculated to increase by 0.02 ± 0.01 $\mu g\ m^{-3}\ K^{-1}$ (5% K^{-1}) whereas for S6, the change is 0.08 $\mu g\ m^{-3}$ (27%). Additionally, IPR analysis shows an increase of 0.06 ± 0.03 $\mu g\ m^{-3}\ K^{-1}$ (1.3%) NO_3^- in the total aerosol process budget (see Section 2.1) within the PBL.

Coarse mode NO_3^- concentrations increase by 0.02 ± 0.02 $\mu g\ m^{-3}\ K^{-1}$ (3% K^{-1}) over the model domain due to increased formation of $NaNO_3$ aerosols. In scenario S6, the change is calculated to be 0.03 $\mu g\ m^{-3}$ (3%). Coarse mode NH_4^+ concentrations decrease by 0.01 ± 0.01 $\mu g\ m^{-3}\ K^{-1}$(−2% K^{-1}), which can be attributed to increased evaporation of ammonia (NH_3) from coarse particles. The IPR analysis shows that the occurrence of the NH_4^+ in the coarse mode within the PBL decreases by 0.038 ± 0.044 $\mu g\ m^{-3}\ K^{-1}$ (1.4%) by physical processes. In addition, less gaseous ammonia is removed by dry deposition as temperatures increase.

4. Conclusions

The aerosol mass concentrations and its chemical composition over the Eastern Mediterranean in July 2004 and the impact of temperature perturbations on them have been simulated using the WRF/CMAQ mesoscale modeling system coupled with the MEGAN biogenic model. Simulations agree with reported observations for the region. The major aerosol component is nss-SO_4^{2-}, particularly in areas downwind of megacities. Urban areas are characterized by high primary OA and undefined fine fraction associated with anthropogenic emissions. Aerosols downwind of significant emission sources contain higher inorganic components than undefined fraction. Sea-salt and dust are also important contributors to PM_{10} in the region.

Simulations showed that increasing temperatures lead to significant reductions in the cloud fractions and in aqueous-phase nss-SO_4^{2-} production. They also result in enhanced biogenic emissions that increase the biogenic SOA formation. However, the decreases in nss-SO_4^{2-} in warmer temperatures seem to counterbalance the increases in OA levels, resulting overall in small spatially-averaged changes in $PM_{2.5}$ levels with temperature (0.003 ± 0.042 μg m^{-3} K^{-1}). It is found that there is a significant spatial variability in the $PM_{2.5}$ response to temperature changes. Larger responses of the PM concentrations are calculated when meteorology changes induced by higher temperatures (like humidity, clouds, precipitation and winds) are also considered.

Our findings are in general agreement with the Dawson et al. (2007) study that focused on the impact of climate or individual meteorological parameters on North America aerosol levels. They found small differences in summer $PM_{2.5}$ levels (0.016 μg m^{-3} K^{-1}) due to changes in temperature by 1.5–4.5 K. However, they calculated an increase in the summer sulfate levels by 0.034 μg m^{-3} K^{-1} whereas in the present study an overall decrease is found. These differences reflect the variability of the response of aerosols to temperature changes in different geographical locations, simulated in the present study for the Eastern Mediterranean and by Carvalho et al. (2010) over Europe.

Under a warmer future climate, PM levels and chemical composition may be subject to significant changes that could contribute to exceedences in the summertime PM levels. Under higher temperatures, the interactions between the fine anthropogenic aerosols from large urban agglomerations and the naturally emitted sea-salt and dust particles can enhance inorganic aerosol components in regions downwind of the urban source areas. Thus, a warmer climate and growing urbanization will result in PM level and chemical composition changes not only in megacities, but also in the surrounding areas.

Acknowledgments

This work has been performed within the CityZen project in the frame of the European Union Seventh Framework Programme (Grant Agreement no. 212095). We thank the National Air Pollution Monitoring Network of the Hellenic Ministry of Environment Energy and Climate Change for the provision of data for Athens, Dr. A. Vavatzanidis for the observational data for Thessaloniki and Prof. I. Vardavas for comments. Regional Emissions were derived from the continental scale EMEP/INERIS inventory provided by G. Siour (LISA/IPSL/INERIS) and B. Bessagnet (INERIS).

Appendix. Supplementary material

Supplementary material associated with this article can be found, in the online version, at doi:10.1016/j.atmosenv.2011.12.044.

References

Arsene, C., Bougiatioti, A., Mihalopoulos, N., 2009. Sources and variability of non-methane hydrocarbons in the Eastern Mediterranean. Global NEST 11 (3), 333–340.

Athanasopoulou, E., Tombrou, M., Pandis, S.N., Russel, A.G., 2008. The role of sea-salt emissions and heterogeneous chemistry in the air quality of polluted coastal areas. Atmospheric Chemistry and Physics 8, 5755–5769.

Bardouki, H., Liakakou, H., Economou, C., Sciare, J., Smolik, J., Zdimal, V., Eleftheriadis, K., Lazaridis, M., Dye, C., Mihalopoulos, N., 2003. Chemical composition of size-resolved atmospheric aerosols in the eastern Mediterranean during summer and winter. Atmospheric Environment 37, 195–208.

Bernard, S.M., Samet, J.M., Grambsch, A., Ebi, K.L., Romieu, I., 2001. The potential impact of climate variability and change on air pollution-related health effects in the United States. Environmental Health Perspectives 109 (Suppl. 2), 199–209.

Binkowski, F.S., Roselle, S.J., 2003. Models-3 community multiscale air quality (CMAQ) model aerosol component: 1. Model description. Journal of Geophysical Research 108 (D6), 4183. doi:10.1029/2001JD001409.

Binkowski, F.S., Shankar, U., 1995. The regional particulate model, 1, Model description and preliminary results. Journal of Geophysical Research 100, 26191–26209.

Byun, D., Schere, K.L., 2006. Review of the governing equations, computational algorithms, and other components of the Models-3 Community Multiscale Air Quality (CMAQ) modeling system. Applied Mechanics Reviews 59, 51–77.

CARB, 2007. Speciation Profiles Used in ARB Modeling. California Air Resources Board, Sacramento, California. http://www.arb.ca.gov/ei/speciate/speciate.htm.

Carlton, A.G., Bhave, P.V., Napelenok, S.L., Edney, E.O., Sarwar, G., Pinder, R.W., Pouliot, G.A., Houyoux, M., 2010. Model representation of secondary organic aerosol in CMAQv4.7. Environmental Science and Technology 44, 8553–8560.

Carvalho, A., Monteiro, A., Solman, S., Miranda, A.I., Borrego, C., 2010. Climate-driven changes in air quality over Europe by the end of the 21st century, with special reference to Portugal. Environmental Science and Policy 13, 445–458.

Dawson, J.P., Adams, P.J., Pandis, S.N., 2007. Sensitivity of $PM_{2.5}$ to climate in the Eastern USA: a modeling case study. Atmospheric Chemistry and Physics 7, 4295–4309.

de Leeuw, G., Neele, F.P., Hill, M., Smith, M.H., Vignati, E., 2000. Production of sea spray aerosol in the surf zone. Journal of Geophysical Research. 105 (D24), 29397–29409.

Dentener, F., Kinne, S., Bond, T., Boucher, O., Cofala, J., Generoso, S., Ginoux, P., Gong, S., Hoelzemann, J.J., Ito, A., Marelli, L., Penner, J.E., Putaud, J.-P., Textor, C., Schulz, M., van der Werf, G.R., Wilson, J., 2006. Emissions of primary aerosol and precursor gases in the years 2000 and 1750 prescribed data-sets for AeroCom. Atmospheric Chemistry and Physics 6, 4321–4344.

Eleftheriadis, K., Balis, D., Ziomas, I., Colbeck, I., Manalis, N., 1998. Atmospheric aerosol and gaseous species in Athens, Greece. Atmospheric Environment 32, 2183–2191.

Foley, K.M., Roselle, S.J., Appel, K.W., Bhave, P.V., Pleim, J.E., Otte, T.L., Mathur, R., Sarwar, G., Young, O.J., Gilliam, C.G., Kelly, J.T., Gilland, A.B., Bash, J.O., 2010. Incremental testing of the Community Multiscale Air Quality (CMAQ) modeling system version 4.7. Geoscientific Model Development 3, 205–226.

Gerasopoulos, E., Kouvarakis, G., Babasakalis, P., Vrekoussis, M., Putaud, J.-P., Mihalopoulos, N., 2006. Origin and variability of particulate matter (PM_{10}) mass concentrations over the Eastern Mediterranean. Atmospheric Environment 40, 4679–4690.

Gong, S.L., 2003. A parameterization of sea-salt aerosol source function for sub- and super-micron particles. Global Biogeochemical Cycles 17 (4), 1097. doi:10.1029/2003GB002079.

Grell, G.A., Peckham, S.E., Schmitz, R., McKeen, S.A., Frost, G., Skamarock, W.C., Eder, B., 2005. Fully coupled "online" chemistry within the WRF model. Atmospheric Environment 39, 6957–6975.

Guenther, A., Karl, T., Harley, P., Wiedinmyer, C., Palmer, P.I., Geron, C., 2006. Estimates of global terrestrial isoprene emissions using MEGAN (Model of Emissions of Gases and Aerosols from Nature). Atmospheric Chemistry and Physics 6, 3181–3210.

Im, U., Markakis, K., Unal, A., Kindap, T., Poupkou, A., Incecik, S., Yenigun, O., Melas, D., Theodosi, C., Mihalopoulos, N., 2010. Study of a winter PM episode in Istanbul using high resolution WRF/CMAQ modeling system. Atmospheric Environment 44, 3085–3094.

Im, U., Markakis, K., Poupkou, A., Melas, D., Unal, A., Gerasopoulos, E., Daskalakis, N., Kanakidou, M., 2011. The impact of temperature changes on summertime ozone and its' precursors in the Eastern Mediterranean. Atmospheric Chemistry and Physics 11, 3847–3864.

IPCC: Climate change, 2007. Synthesis Report, Intergovernmental Panel on Climate Change.

Jacob, D.J., Winner, D.A., 2009. Effect of climate change on air quality. Atmospheric Environment 41, 51–63.

Jimenez, J.L., Canagaratna, M.R., Donahue, N.M., Prevot, A.S.H., Zhang, Q., Kroll, J.H., DeCarlo, P.F., Allan, J.D., Coe, H., Ng, N.L., Aiken, A.C., Docherty, K.S., Ulbrich, I.M., Grieshop, A.P., Robinson, A.L., Duplissy, J., Smith, J.D., Wilson, K.R., Lanz, V.A., Hueglin, C., Sun, Y.L., Tian, J., Laaksonen, A., Raatikainen, T., Rautiainen, J., Vaattovaara, P., Ehn, M., Kumala, M., Tomlinson, J.M., Collins, D.R., Cubison, M.J., Dunlea, E.J., Huffman, J.A., Onasch, T.B., Alfarra, M.R., Williams, P.I., Bower, K., Kondo, J., Schenider, J., Drewnick, F., Borrmann, S., Weimer, S., Demerjian, K., Salcedo, D., Cottrell, L., Griffin, R., Takami, A., Miyoshi, T., Hatakeyama, S., Shimono, A., Sun, J.Y., Zhang, Y.M., Dzepina, K., Kimmel, J.R., Sueper, D., Jayne, J.T., Herndon, S.C., Trimborn, A.M., Williams, L.R., Wood, E.C., Middlebrook, A.M., Kolb, C.E., Baltensperger, U., Worsnop, D.R., 2009. Evolution of organic aerosols in the atmosphere. Science 326 (5959), 1525–1529.

Kanakidou, M., Mihalopoulos, N., Kindap, T., Im, U., Vrekoussis, M., Gerasopoulos, E., Dermitzaki, E., Unal, A., Kocak, M., Markakis, K., Melas, D., Kouvarakis, G., Youssef, A.F., Richter, A., Hatzianastassiou, N., Hilboll, A., Ebojie, F., von Savigny, C., Ladstaetter-Weissenmayer, A., Burrows, J., Moubasher, H., 2011. Megacities as hot spots of air pollution in the East Mediterranean. Atmospheric Environment 45, 1223–1235.

Karanasiou, A., Moreno, T., Amato, F., Lumbreras, J., Narros, A., Borge, R., Tobias, A., Boldo, E., Linares, C., Pey, J., Reche, C., Alastuey, A., Querol, X., 2011. Road dust contribution to PM levels-Evaluation of the effectiveness of street washing activities by means of Positive Matrix Factorization. Atmospheric Environment 45 (2193), 2201.

Kelly, J.T., Bhave, P.V., Nolte, C.G., Shankar, U., Foley, K.M., 2010. Simulating emissions and chemical evolution of coarse sea-salt particles in the Community Multiscale Air Quality (CMAQ) model. Geoscientific Model Development 3, 257–273.

Koçak, M., Kubilay, N., Mihalopoulos, N., 2004. Ionic composition of lower tropospheric aerosols at a Northeastern Mediterranean site: implications regarding sources and long-range transport. Atmospheric Environment 38, 2067–2077.

Koçak, M., Mihalopoulos, N., Kubilay, N., 2007. Chemical composition of the fine and coarse aerosols in the northeastern Mediterranean. Atmospheric Environment 41, 7351–7368.

Koçak, M., Theodosi, C., Zarmpas, P., Im, U., Bougiatioti, A., Yenigun, O., Mihalopoulos, N., 2011. Particulate matter (PM_{10}) in Istanbul: origin, sources and potential impact on surrounding regions. Atmospheric Environment 45, 6891–6900.

Koulouri, E., Saarikoski, S., Theodosi, C., Markaki, Z., Gerasopoulos, E., Kouvarakis, G., Makela, T., Hillamo, R., Mihalopoulos, N., 2008. Chemical composition and sources of fine and coarse aerosol particles in the Eastern Mediterranean. Atmospheric Environment 42, 6542–6550.

Kouvarakis, G., Mihalopoulos, N., 2002. Seasonal variation of dimethylsulfide in the gas phase and of methanosulfate and non-sea-salt sulfate in the aerosol phase in the Eastern Mediterranean atmosphere. Atmospheric Environment 36, 929–938.

Lazaridis, M., Spyridaki, A., Solberg, S., Smolik, J., Zdimal, V., Eleftheriadis, E., Aleksandropoulou, V., Hov, O., Georgopoulos, P.G., 2005. Mesoscale modeling of combined aerosol and photo-oxidant processes in the Eastern Mediterrnean. Atmospheric Chemistry and Physics 5, 927–940.

Lelieveld, J., Berresheim, H., Borrmann, S., Crutzen, P.J., Dentener, F.J., Fischer, H., Feichter, J., Flatau, P.J., Heland, J., Holzinger, R., Korrmann, R., Lawrance, M.G., Levin, Z., Markowiz, K.M., Mihalopoulos, N., Minikin, A., Ramanathan, V., de Reus, M., Roelofs, G.J., Scheeren, H.A., Sciare, J., Schlager, H., Schultz, M., Siegmund, P., Steil, B., Stephanou, E.G., Stier, P., Traub, M., Warneke, C., Williams, J., Ziereis, H., 2002. Global air pollution crossroads over the Mediterranean. Science 298, 794–799.

Matthias, V., Aulinger, A., Quante, M., 2008. Adapting CMAQ to investigate air pollution in North Sea coastal regions. Environmental Modelling and Software 23, 356–368.

Mihalopoulos, N., Stephanou, E., Kanakidou, M., Pilitsidis, S., Bousquet, P., 1997. Tropospheric aerosol ionic composition in the Eastern Mediterranean region. Tellus 49B, 314–326.

Mihalopoulos, N., Kerminen, V.M., Kanakidou, M., Berresheim, K., Sciare, J., 2007. Formation of particulate sulfur species (sulfate and methanosulfate) during summer over the Eastern Mediterranean: a modeling approach. Atmospheric Environment 41, 6860–6871.

Mitsakou, C., Kallos, G., Papantoniou, N., Spyrou, C., Solomos, S., Astitha, M., Housiadas, C., 2008. Saharan dust levels in Greece and received inhalation doses. Atmospheric Chemistry and Physics 8, 7181–7192.

Myriokefalitakis, S., Vrekoussis, M., Tsigaridis, K., Wittrock, F., Richter, A., Bruhl, C., Volkamer, R., Burrows, J.P., Kanakidou, M., 2008. The influence of natural and anthropogenic secondary sources on the glyoxal global distribution. Atmospheric Chemistry and Physics 8, 4965–4981.

Myriokefalitakis, S., Vignati, E., Tsigaridis, K., Papadimas, C., Sciare, J., Mihalopoulos, N., Facchini, M.C., Rinaldi, M., Dentener, F.J., Ceburnis, D., Hatzianastasiou, N., O'Dowd, C., van Meele, M., Kanakidou, M., 2010. Global modeling of the oceanic source of organic aerosols. Advances in. Meteorology. doi:10.1155/2010/939171.

Nenes, A., Pandis, S.N., Pilinis, C., 1998. ISORROPIA: a new thermodynamic equilibrium model for multiphase multicomponent inorganic aerosols. Aquatic Geochemistry 4 (1), 123–152.

Nicolas, J., Chiari, M., Crespo, J., Orellana, I.G., Lucarelli, F., Nava, S., Pastor, C., Yubero, E., 2008. Quantification of Saharan and local dust impact in an arid Mediterranean area by the positive matrix factorization (PMF) technique. Atmospheric Environment 42, 8872–8882.

Otte, T.L., Pleim, J.E., 2010. The meteorology-chemistry Interface Processor (MCIP) for the CMAQ modeling system: updates through MCIPv3.4.1. Geoscientific Model Development 3, 243–256.

Papanastasiou, D.K., Poupkou, A., Katragkou, E., Amiridis, V., Melas, D., Mihalopoulos, N., Basart, S., Pérez, C., Baldasano, J.M., 2010. An assessment of the efficiency of dust regional modelling to predict Saharan dust transport episodes. Advances In Meteorology, 9. doi:10.1155/2010/154368. Article ID 154368.

Schwartz, J., Dockery, D.W., Neas, L.M., 1996. Is daily mortality associated specifically with fine particles? Journal of Air and Waste Management Association 46, 927–939.

Seinfeld, J.H., Pandis, S.N., 2006. Atmospheric Chemistry and Physics: From Air Pollution to Climate Change, third ed. John Wiley, New York.

Sillanpaa, M., Hillamo, R., Saarikoski, S., Frey, A., Pennanen, A., Makkonen, U., Spolnik, Z., Grieken, R.V., Branis, M., Brunekreef, B., Chalbot, M.-C., Kuhlbusch, T., Sunyer, J., Kerminen, V.-M., Kulmala, M., Salonen, R.O., 2006. Chemical composition and mass closure of particulate matter at six urban sites in Europe. Atmospheric Environment 40, S212–S223.

Skamarock, W.C., Klemp, J.B., 2008. A time-split non-hydrostatic atmospheric model. Journal of Computational Physics 227, 3465–3485.

Smolik, J., Zdimal, V., Schwarz, J., Lazaridis, M., Havranek, V., Eleftheriadis, K., Mihalopoulos, N., Bryant, C., Colbeck, I., 2003. Size resolved mass concentration and elemental composition of atmospheric aerosols over the Eastern Mediterranean area. Atmospheric Chemistry and Physics 3, 2207–2216.

Terzi, E., Argyropoulos, G., Bougatioti, A., Mihalopoulos, N., Nikolaou, K., Samara, C., 2010. Chemical composition and mass closure of ambient PM10 at urban sites. Atmospheric Environment 44, 2231–2239.

Theodosi, C., Im, U., Bougiatioti, A., Zarmpas, P., Yenigun, O., Mihalopoulos, N., 2010. Aerosol chemical composition over Istanbul. Science of the Total Environment 408 (12), 2482–2491.

Tsigaridis, K., Kanakidou, M., 2007. Secondary organic aerosol importance in the future atmosphere. Atmospheric Environment 41 (22), 4682–4692.

Tsigaridis, K., Lathiere, J., Kanakidou, M., Hauglustaine, D.A., 2005. Naturally driven variability in the global secondary organic aerosol over a decade. Atmospheric Chemistry and Physics 5, 1891–1904.

Tsitouridou, R., Voutsa, D., Kouimtzis, T., 2003. Ionic composition of PM_{10} in the area of Thessaloniki, Greece. Chemosphere 52, 883–891.

Whitby, K.T., 1978. The physical characteristics of sulfur aerosols. Atmospheric Environment 12, 135–159.

Zhang, K.M., Knipping, E.M., Wexler, A.S., Bhave, P.V., Tonnesen, G.S., 2005. Size distribution of sea-salt emissions as a function of relative humidity. Atmospheric Environment 39, 3373–3379.